

Avoided level crossing, correlation and entanglement of two-component Bose-Einstein condensates in a double well

Weibin Li,^{1,2,*} Wenxing Yang,^{1,2} Xiaotao Xie,³ Jiahua Li,³ and Xiaoxue Yang³

¹*State Key Laboratory of Magnetic Resonance and Atomic and Molecular Physics, Wuhan Institute of Physics and Mathematics, Chinese Academy of Sciences, Wuhan 430071, Peoples Republic of China*

²*Graduate school, Chinese Academy of Sciences, Beijing 10080, Peoples Republic of China*

³*Department of Physics, Huazhong University of Science and Technology, Wuhan 430074, People's Republic of China*

We consider a novel system of two-component atomic Bose-Einstein condensate in a double-well potential. Based on the well-known two-mode approximation, we demonstrate that there are obvious avoided level-crossings when both interspecies and intraspecies interactions of two species are increased. The quantum dynamics of the system exhibits revised oscillating behaviors compared with a single component condensate. We also examine the entanglement of two species. Our numerical calculations show the onset of entanglement can be signed as a violation of Cauchy-Schwarz inequality of second-order cross correlation function. Consequently, we use Von Neumann entropy to quantify the degree of entanglement.

PACS numbers: 03.75.Gg, 05.30.Jp, 03.75.Lm, 03.75.Mn

I. INTRODUCTION

The study of Bose-Einstein condensates (BECs) immersed in artificial optical lattices has become one of several focuses of current interest in the ongoing exploration of the ultralow temperature physics [1]. Recently, experiments of the superfluid to Mott-insulator transition [2] and the number squeezing related to quantum optics [3] have been realized. They strikingly open the possibility to study fundamental many-body physics with highly controllable parameters [1, 4], as well as find the potential applications in quantum information processing [5, 6]. In particular, one may prefer to study the double well system, for which is considered as the simplest many lattice model [4, 7, 8]. The essential underlying physics can be understood within the study of a double-well BECs with a variable barrier height in the two-mode approximation [9, 10, 11] and many rich strongly correlated quantum properties of condensates, such as squeezing [10, 12], the self-trapping of Josephson oscillations [13, 14, 15, 16], the collapse and revivals dynamics [17], entanglement [18], and spectra [19, 20] have been examined.

On the other hand, experimental realization of multi-component BECs [21, 22, 23] has stimulated considerable interests in the study of storing BECs in lattices when the interspecies interaction of the mixed multi-component BECs affects the quantum tunnel and quantum coherence crucially [24, 25, 26]. Examples include both the experiment demonstrating of coherent transport of multi-component BECs in optical lattices [27] and theoretical predications of coexisting superfluid and Mott phases [28], fragmented condensates with topological excitations [29], maximally entangled atomic states [30], dimer phases [31], and heteronuclear molecular BECs [32, 33]. However, the research of multi-component BECs in the double-well has just begin. Ashhab et.al. [34] studied the Josephson junction between two spatially separated condensates with a hyperfine degree of freedom. They find in the semiclassical limitation the dynamics of the system can be described by the Bloch equations [34]. Recently, Ng and co-workers studied the double-well tunnelling of two-component BECs [35] and pointed out the generation of quantum entanglement of different modes. As a counterpoint, the entangling property in the weak-coupling regime with large number of atoms is also studied [36]. It reveals that the atoms of two components initially separately localized in the different potential wells can tunnel as entangled pairs when the interspecies interactions are strong enough. These schemes are of particular interest for engineering many-particle entanglement in BECs, which may play a prominent role in the study of quantum computing and quantum information [36]. Up to now we have only a limited idea about the properties of two-component BECs in a double-well compared with the single component system. In addition, other aspects, such as spectra and quantum dynamics, have not been specified. Thus a systematic examination is required.

In this paper, we pay much attention to some significant issues of the two-component BECs in double-well. At first we put forward an algebra approach to calculate the eigenenergy and eigenstate explicitly based on the two-mode approximation. It is simple and can be coded by a several-line mathematica program. By this, it is surprised to find

*Electronic address: weibinli@wipm.ac.cn

the onset of obviously avoided level-crossing [37]. This may have profound impacts on the double-well systems and may relate certain kind of chaotic behaviors [37]. With the eigenspectra and eigenstate, we study the dynamics in section III. Rabi oscillation and self-trapping effect [13] are demonstrated with different initial conditions. In section IV, the correlation and entanglement of the system are examined especially in two limiting cases [35, 36]. We show Von Neumann entropy are always nonzero whether apparent entanglement is triggered. However the violation of Cauchy-Schwarz inequality of second-order cross correlation function can indicates the entrance of entanglement. We conclude in section V.

II. QUANTUM TWO-MODE MODEL

A. Model Hamiltonian

The many-body Hamiltonian of atomic BECs in a external potential $V(r)$, in second quantization, is [13]

$$\hat{H} = \int d\mathbf{r} \hat{\Psi}^\dagger(\mathbf{r}) \left[-\frac{\hbar^2}{2m} \nabla^2 + V(\mathbf{r}) \right] \hat{\Psi}(\mathbf{r}) + \frac{g}{2} \int d\mathbf{r} \hat{\Psi}^\dagger(\mathbf{r}) \hat{\Psi}^\dagger(\mathbf{r}) \hat{\Psi}(\mathbf{r}) \hat{\Psi}(\mathbf{r}) \quad (1)$$

where $\hat{\Psi}(\mathbf{r})$ and $\hat{\Psi}^\dagger(\mathbf{r})$ are the bosonic annihilation and creation field operators, m is the particle mass, and $g = (4\pi a_s \hbar^2)/m$, where a_s is the s-wave scattering length. In studies of double-well BECs, one may prefer to use the well-known two-mode approximation [9, 10, 11] to capture the essential physics. We study a two-component BECs trapped in a symmetric double-well potential. The total number of atoms in components A and B of the condensate are N_a and N_b , respectively. With this approximation and the conservation of the particle number of each component, the system is described by the Hamiltonian ($\hbar = 1$) [35, 36],

$$\begin{aligned} \hat{H} = & \frac{\Omega_a}{2} (\hat{a}_L^\dagger \hat{a}_R + \hat{a}_R^\dagger \hat{a}_L) + \frac{\Omega_b}{2} (\hat{b}_L^\dagger \hat{b}_R + \hat{b}_R^\dagger \hat{b}_L) + \kappa (\hat{a}_L^\dagger \hat{a}_L \hat{b}_L^\dagger \hat{b}_L \\ & + \hat{a}_R^\dagger \hat{a}_R \hat{b}_R^\dagger \hat{b}_R) + \frac{\kappa_a}{2} [(\hat{a}_L^\dagger \hat{a}_L)^2 + (\hat{a}_R^\dagger \hat{a}_R)^2] \\ & + \frac{\kappa_b}{2} [(\hat{b}_L^\dagger \hat{b}_L)^2 + (\hat{b}_R^\dagger \hat{b}_R)^2] \end{aligned} \quad (2)$$

where the subscripts L and R denote localized modes in the left and right potential wells. $\hat{a}_j^\dagger(\hat{a}_j)$ and $\hat{b}_j^\dagger(\hat{b}_j)$ are, respectively, the creation (annihilation) operators of components A and B residing in the j th well, $j = L, R$. The parameters $\Omega_a(\Omega_b)$, $\kappa_a(\kappa_b)$ and κ describe the tunnelling rate, self-interaction strength of component A (B) and the interspecies interaction strength.

B. Procedure for the Eigenvalue Equation

Although there are continuous interests in the study of the Hamiltonian (2) [34, 35, 36, 38], with the result that such systems may provide a potential entanglement regime of macroscopic ensembles, no one seems to have been able to obtain the eigenspectra systemically even for a small number of atoms [35]. In handling the system with nonlinear interactions among several boson modes, one usually needs to use the well-known Bethe ansatz [40] on the energy eigensates with several parameters determined by highly complicated reduced system of Bethe equations. In this section, we shall utilize an efficient and simple method [20, 39] to solve Hamiltonian (2). We show that the corresponding eigenvalue can be reduced into a differential equation and thus solved by a simple MATHEMATICA code.

The eigenvalue equation for the Hamiltonian (2),

$$\hat{H} |\Psi_{E, N_a, N_b}\rangle = E |\Psi_{E, N_a, N_b}\rangle \quad (3)$$

Denote the energy eigenstates as

$$\begin{aligned} |\Psi_{E, N_a, N_b}\rangle &= \hat{F}(\hat{a}_L^\dagger, \hat{a}_R^\dagger; \hat{b}_L^\dagger, \hat{b}_R^\dagger) |\text{vac}\rangle_A |\text{vac}\rangle_B \\ &= \hat{F}(\hat{a}_L^\dagger, \hat{a}_R^\dagger; \hat{b}_L^\dagger, \hat{b}_R^\dagger) |\text{vac}\rangle_{A, B} \end{aligned} \quad (4)$$

where F is a polynomial of the creation operators $\hat{a}_{L,R}^\dagger$ and $\hat{b}_{L,R}^\dagger$. The vacuum state $|\text{vac}\rangle_S = |p=0, q=0\rangle_S$ denotes a Fock state of species S ($S = A, B$) without any bosons in the left well and right well. Throughout the following paper, states $|p, q\rangle_S$ denote Fock states with p atoms of species S ($S = A, B$) in the left well and q atoms of species S ($S = A, B$) in the right well. Noting $\hat{H}\hat{F}|\text{vac}\rangle_{A,B} = ([\hat{H}, \hat{F}] + \hat{F}\hat{H})|\text{vac}\rangle_{A,B}$ due to the fact $\hat{H}|\text{vac}\rangle_{A,B} = 0$, the eigenvalue equation becomes $([\hat{H}, \hat{F}] - E\hat{F})|\text{vac}\rangle_{A,B} = 0$. Finally, by using the identities $\alpha_j|\text{vac}\rangle_{A,B} = 0$, $[\hat{\alpha}_j^\dagger, \hat{F}] = 0$, $[\hat{\alpha}_j, \hat{F}] = \partial\hat{F}/\partial\hat{\alpha}_j^\dagger$ ($\alpha = a, b$), it is then straightforward to show that the polynomial \hat{F} of creation operators $\hat{\alpha}_{L,R}^\dagger$, ($\alpha = a, b; j = L, R$) satisfies the operator-type differential equation as follows:

$$\begin{aligned} & \left[\frac{\Omega_a}{2} \left(x_1 \frac{\partial}{\partial x_2} + x_2 \frac{\partial}{\partial x_1} \right) + \frac{\Omega_b}{2} \left(y_1 \frac{\partial}{\partial y_2} + y_2 \frac{\partial}{\partial y_1} \right) \right. \\ & + \frac{\kappa_a}{2} \left(x_1^2 \frac{\partial^2}{\partial x_1^2} + x_2^2 \frac{\partial^2}{\partial x_2^2} \right) + \frac{\kappa_b}{2} \left(y_1^2 \frac{\partial^2}{\partial y_1^2} + y_2^2 \frac{\partial^2}{\partial y_2^2} \right) \\ & \left. + \kappa \left(x_1 y_1 \frac{\partial^2}{\partial x_1 \partial y_1} + x_2 y_2 \frac{\partial^2}{\partial x_2 \partial y_2} \right) \right] F = \lambda F \end{aligned} \quad (5)$$

where we have used the convenient notations $x_{1,2} \equiv \hat{a}_{L,R}$, $y_{1,2} \equiv \hat{b}_{L,R}$. And F is a polynomial of the form $F(x_1, x_2, y_1, y_2) = \sum_{n=0}^{N_a} \sum_{m=0}^{N_b} c_{n,m} x_1^n x_2^{N_a-n} y_1^m y_2^{N_b-m}$. The parameter λ relates to the energy eigenvalues by

$$\lambda = E - \left(\frac{\kappa_a}{2} N_a + \frac{\kappa_b}{2} N_b \right) \quad (6)$$

It is important to note that the operator-type differential equation (5) can formally be regarded as a c -number differential equation owing to the result that all the operators are mutually commutable with each other and hence can be solved by any ordinary way [20, 39].

Substituting the c -number polynomial $F(x_1, x_2, y_1, y_2)$ into the differential equation (5), we find the eigenvalues can be calculated by solving the matrix equation

$$M\sigma = \lambda\sigma \quad (7)$$

where σ is a D -dimension column vector, $D = (N_a + 1) \times (N_b + 1)$ and M is a square matrix of order D with the matrix elements $M_{k,l;m,n} = \Omega_a/2[(N_a - k)\delta_{k,l-1} + k\delta_{k,l+1}]\delta_{m,n} + \Omega_b/2[(N_b - m)\delta_{m,n-1} + m\delta_{m,n+1}]\delta_{k,l} + \{\kappa_a/2[k(k-1) + (N_a - k)(N_a - k - 1)] + \kappa_b/2[m(m-1) + (N_b - m)(N_b - m - 1)] + \kappa[mk + (N_a - k)(N_b - m)]\}\delta_{k,l}\delta_{m,n}$. To obtain the eigenvalues of vector σ , we can express the matrix M by a MATHEMATICA code and thus diagonalize it directly [41].

C. Avoided Level-crossing

We have given a systematical procedure to calculate the eigenenergy and eigenstates in term of parameter λ by solving either analytically or numerically Eq. (14). For example, one can obtain explicit results of the simplest case $N_a = N_b = 1$, which is similar to the results in [35]. Noting here λ is related to eigenenergy by Eq.(6). We don't plan on listing these results due to the large number of eigenvalues ($D = (N_a + 1) \times (N_b + 1)$). One can validate the efficiency of the method using the code [41].

The spectra of such systems are usually intricate functions of the parameters involved in the Hamiltonian (2). To address the details of spectra for given N_a and N_b , we shall plot all of the spectra. For convenience, we make $\Omega_a = \Omega_b = \Omega$ and $\kappa_a = \kappa_b = \kappa$. It is a good approximation to ^{87}Rb condensate of atoms in hyperfine spin states $|F=2, M_f=1\rangle$ and $|F=1, m_f=-1\rangle$ with similar scattering lengths [22]. Hereafter we consider only $u \equiv \kappa/\Omega > 0$, i.e. the repulsive situation. All $D = (N_a + 1) \times (N_b + 1)$ eigenvalues are depicted in FIG.1 (top) for $N_a = N_b = 5$. In cases of $\Omega \gg \kappa$ and $\Omega \ll \kappa$ most of the eigenstates remain nearly degenerate. The property of degenerate can be well understood in the Schwinger representation. Defining angular-momentum operators of two boson modes of each component as

$$\begin{aligned} \hat{J}_{\alpha x} &= \frac{1}{2}(\hat{\alpha}_L^\dagger \hat{\alpha}_L - \hat{\alpha}_R^\dagger \hat{\alpha}_R) \\ \hat{J}_{\alpha y} &= \frac{1}{2i}(\hat{\alpha}_L^\dagger \hat{\alpha}_R - \hat{\alpha}_R^\dagger \hat{\alpha}_L) \\ \hat{J}_{\alpha z} &= \frac{1}{2}(\hat{\alpha}_L^\dagger \hat{\alpha}_R + \hat{\alpha}_R^\dagger \hat{\alpha}_L) \end{aligned} \quad (8)$$

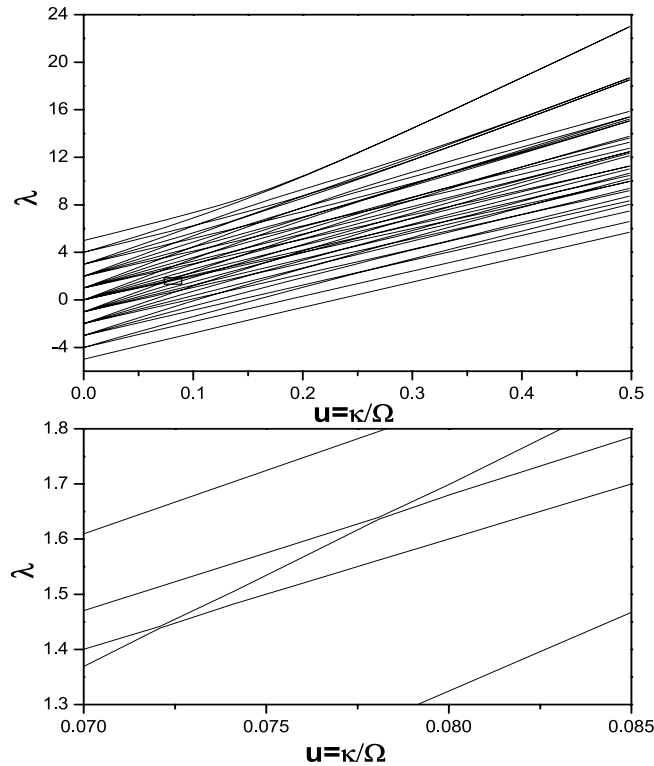


FIG. 1: Level for $N_a = N_b = 5$. The bottom is the enlargement of rectangle in the top part, which shows avoided level crossing.

where $\alpha = a, b$. Here $\hat{\mathbf{J}}_\alpha = (\hat{J}_{\alpha x}, \hat{J}_{\alpha y}, \hat{J}_{\alpha z})$ are the usual angular momentum operators. Denote $|j_\alpha, m_\alpha\rangle$ the eigenstates of $\hat{J}_\alpha^2 = \hat{J}_{\alpha x}^2 + \hat{J}_{\alpha y}^2 + \hat{J}_{\alpha z}^2$ and $\hat{J}_{\alpha z}$ with $\hat{J}_\alpha^2 |j_\alpha, m_\alpha\rangle = j_\alpha(j_\alpha + 1) |j_\alpha, m_\alpha\rangle$ and $\hat{J}_{\alpha z} |j_\alpha, m_\alpha\rangle = m_\alpha |j_\alpha, m_\alpha\rangle$, where $j_\alpha = N_\alpha/2$. Thus the Hamiltonian (2) may be written [36]

$$\hat{H} = \Omega \hat{J}_z + \kappa \hat{J}_x^2 \quad (9)$$

where $\hat{\mathbf{J}} = \hat{\mathbf{J}}_a + \hat{\mathbf{J}}_b$ is the total angular momentum of the system. It is interesting to note that Hamiltonian (9) looks same as the Hamiltonian of single component BECs in a double-well [9]. The spectra suggests that for Ω big the first term in Hamiltonian (9) dominates, in which case the energy eigenstates are close to the eigenstates of \hat{J}_z . Since $m_\alpha = -j_\alpha, -j_\alpha - 1, \dots, j_\alpha - 1, j_\alpha$, the eigenvalues of j_z are $m = -(j_a + j_b), -(j_a + j_b) + 1, \dots, (j_a + j_b) - 1, (j_a + j_b)$. Corresponding degeneracies are $1, 2, \dots, (N_a + N_b)/2, (N_a + N_b)/2 + 1, (N_a + N_b)/2, \dots, 2, 1$. This can be seen obviously in FIG. (1). While for sufficient big u , the system is dominated by the second term of Hamiltonian (9). This means that the eigenstates of the Hamiltonian are close to the eigenstates of \hat{J}_x^2 . From Eq.(8), the operator $\hat{J}_{\alpha x}$ gives the particle number difference of each well for one component. So $\hat{J}_x = \hat{J}_{ax} + \hat{J}_{bx}$ will have the eigenvalues $-(j_a + j_b), -(j_a + j_b) + 1, \dots, (j_a + j_b) - 1, j_a + j_b$. Hamiltonian (9) is symmetric under transformation $\hat{J}_x \rightarrow -\hat{J}_x$ which results in the eigenvalues $0, 1, \dots, (j_a + j_b)^2$ with corresponding degeneracies $j_a + j_b, (j_a + j_b) - 2, \dots, 4, 2$. Although the complete degenerates are not plotted in FIG. (1), we can note the trend which demonstrates the constriction of eigenvalues when κ increases. It is important to note the ground state is not degenerated with respect to u in a large range. This feature means that the ground state is very stable and hard to be excited to the excited states.

What appears interesting as the eigenstates undergo a series of apparent avoided level-crossings in a region of u bounded by the rectangle. The enlargement plot given in bottom of FIG. (1), reveals the characteristic double cone structure of the avoided level crossing. In the intermediate range of u , Both the tunnelling Ω and the interaction κ influence the Hamiltonian. The competition between them is much complicated. The authors [42] have shown the generation of erratic level crossings, where the system contains only a single component BECs in a double-well. It is striking that our system shows apparent avoided level crossings. They are similar to the level repulsion of a interacting boson model addressed in [43], in which the level repulsion characterizes certain quantum phase transition. However, it remains to be explored whether the avoided level-crossings may indicate certain kind of chaotic behaviors or quantum phase transition. This will be subject of our future investigations.

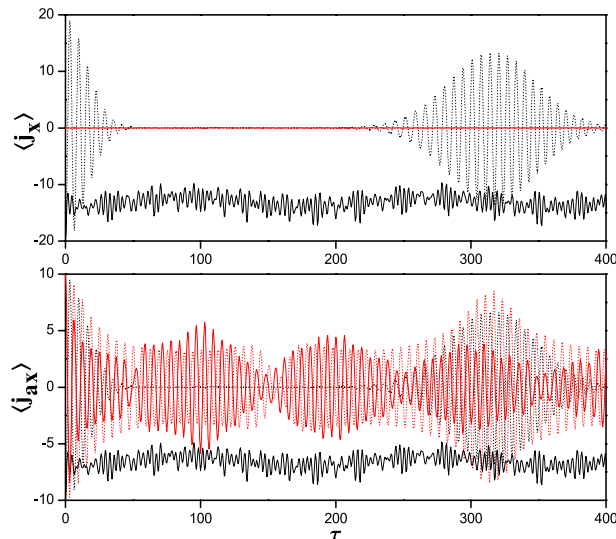


FIG. 2: Dynamics of number differences. The top and the bottom are the mean values of \hat{j}_x and \hat{j}_{ax} for two initial conditions $|j, -j\rangle$ (black) and $|j, 0\rangle$ (red). Here $\Omega = 1.0$, $\tau = \Omega t$ and $\kappa N = 2.5$ for solid curves and $\kappa N = 0.8$ for dotted curves.

III. QUANTUM DYNAMICS ANALYSIS

With the formal development at hand, we now turn to a discussion of the quantum dynamics of this system. The prominent properties of quantum tunnelling dynamics of BECs trapped in a double well depend on the initial conditions and the relative values of tunnelling rate and interaction strength [13, 14, 15, 16]. For single-component condensates, many studies [13, 14, 15, 16] have shown that a self-trapping mechanism can restrict the tunnelling rate significantly due to the two-body interactions. However, the dynamics of two-component BECs is effected by two kinds of interactions, i.e. intraspecies and interspecies interactions. Although previous study [35] reveals the paired tunnelling occurs as interspecies interaction increases, which considers a situation that the atoms of two components are separately prepared in different traps initially, a thorough study of quantum dynamics is not addressed. For example, how the dynamical behaviors of each component and whole system are influenced by intraspecies and interspecies interactions is not studied. In the following, by varying the parameters, we will examine the quantum dynamics of such system.

First of all, we determine the quantum dynamics of Hamiltonian (9), which has the critical relation, $\kappa N = 2\Omega$ [9] with $N = N_a + N_b$ the total number of particles. It is very simple and can be constructed by the standard method [9]. Usually, one calculates the Heisenberg equations of motion

$$\begin{aligned} \frac{d\hat{J}_x}{dt} &= -\Omega\hat{J}_y \\ \frac{d\hat{J}_y}{dt} &= \Omega\hat{J}_x - \kappa(\hat{J}_z\hat{J}_x + \hat{J}_x\hat{J}_z) \\ \frac{d\hat{J}_z}{dt} &= \kappa(\hat{J}_y\hat{J}_x + \hat{J}_x\hat{J}_y) \end{aligned} \quad (10)$$

By representing states of the Hamiltonian (9) in the basis of \hat{J}_z , the time evolution can be obtained by integrating the Schrödinger equation. With the procedure developed in previous section, this work can also be accomplished immediately. Expressing the eigenstate of Hamiltonian (9) as

$$|\Psi_{E, N_a, N_b}\rangle = \sum_{n=0}^{N_a} \sum_{m=0}^{N_b} c_{n,m} |n, N_a - n\rangle_A |m, N_b - m\rangle_B \quad (11)$$

To study the dynamics of Hamiltonian (9) with a initial condition $|\Phi(0)\rangle$, we write down the time dependent state function as

$$|\Phi(t)\rangle = e^{-iHt} |\Phi(0)\rangle \quad (12)$$

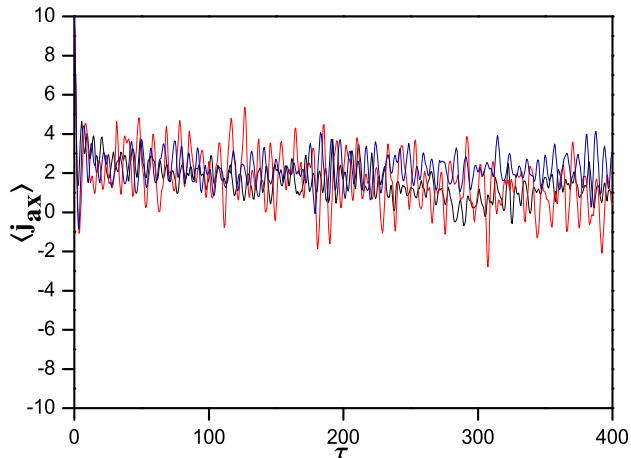


FIG. 3: Number differences for component A with initial state $|j, 0\rangle \equiv |j_a, j_a\rangle_A |j_b, -j_b\rangle_B$. Here black curve represents the case $\Omega = 5.3, \kappa = 1.2$, orange, $\Omega = 1.2, \kappa = 5.0$ and blue, $\Omega = 0.1, \kappa = 4.0$.

With the eigenstate $|\Psi_{E, N_a, N_b}\rangle$, we can obtain

$$|\Phi(t)\rangle = \sum_{l=0}^D e^{-iE_l t} \langle \Psi_l | \Phi(0) \rangle |\Psi_l\rangle \quad (13)$$

where $|\Psi_l\rangle \equiv |\Psi_{E_l, N_a, N_b}\rangle$, $c_{n,m}$ and E_l can be obtained by our method numerically.

We take case $N_a = N_b = 20$, with $\kappa N/\Omega = 2.5$ and $\kappa N/\Omega = 0.8$, corresponding to above and below the threshold. For simplicity, we make $\Omega = 1.0$ and normalize the time in units of single particle tunneling period, $\tau = \Omega t$ in the numerical experiments. In FIG. (2) we plot the mean values of \hat{J}_x (top), which represents the occupation difference of two wells, for two initial states $|j, -j\rangle \equiv |j_a, -j_a\rangle_A |j_b, -j_b\rangle_B$ and $|j, 0\rangle \equiv |j_a, j_a\rangle_A |j_b, -j_b\rangle_B$ with $j = j_a + j_b$. The former means the atoms of both components are prepared in one well initially and the latter corresponds to separately prepare each component in individual well. It is not surprised that the distribution of particles of the latter case is zero. Thus we focus on examining the evolution with initial state $|j, -j\rangle$. During long times, the quantum dynamics of two-component and single component are similar [9]. Below threshold, the dynamics oscillates with revivals at latter times. While above threshold, the revivals don't appear. It can be regarded as the self-trapping [13] of two-component BECs. More interesting, however, is the reversed oscillating properties below and above threshold compared with the single component ones' [9]. Here the revival and oscillation are quite regular below threshold while above threshold the mean values are fluctuated irregularly around constants (depending on the relative values of κ , N and Ω).

To obtain more insight of the dynamics, we also plot the number difference of component A in FIG. (2) (bottom). It is obvious the dynamics of each component is similar to the one of whole system with initial condition $|j, -j\rangle$. The red curves show that although each component oscillates between two wells rapidly when the system is separately prepared, the number of atoms in every well is equal.

On the other hand, when varying Ω and κ , the levels undergo distinguished behaviors, as depicted in FIG (1). One may prefer to study the dynamics within the regime $\kappa/\Omega \gg 1$ or $\kappa/\Omega \ll 1$. We have done the numerical experiments in these region and found for the symmetric situations, i.e. $\Omega_a = \Omega_b = \Omega$ and $\kappa_a = \kappa_b = \kappa$ considered above, they are trivial. In spite of that, the corresponding properties of correlation and entanglement are crucial. We will address these in the following section.

Another interesting phenomenon is self-trapping effect of individual component. As we have shown, it can only happen above threshold when the particles are prepared in a single well initially. Below threshold or evolving from state $|j, 0\rangle$ at $t = 0$ it will not occurs. This is true for the symmetric situation. However when the system contains two kinds of atoms (such as ^{41}K and ^{87}Rb [44]) or the interspecies interaction of these two-component BECs is varied by the application of magnetic control [45], this effect will happen for individual components. Our numerical studies demonstrate it becomes obvious when the tunneling $\Omega_a = \Omega_b = \Omega$ are not equal to the interactions $\kappa_a = \kappa_b = \kappa$ and at the same time at least one of them (Ω and κ) should be above threshold. In FIG (3), we have plot some of

the results. It appears that the atoms of each components are favor to stay in the original wells with time. If we increase the difference between Ω and κ (both above threshold), the self-trapping of individual components become more distinct. While one of them below threshold, it will demand the difference much greater to trigger the effects.

IV. QUANTUM CORRELATION AND ENTANGLEMENT

A particularly striking aspect of the present study is that it allows one to obtain quantum correlations between components. The correlated states of BECs in a double-well model have been a most active research areas, for which open the opportunity to create many-particle entanglement in macroscopic systems [30, 35, 36, 46, 47]. You [30] proposed a scheme to create maximal entangled cluster states starting from a Mott insulator state. Micheli et. al. [46] studied the possibility to create dynamically many-particle entanglement of a two-component BECs. They found within a very short time scale (proportional to $1/N$ with N the number of condensate particles), the entangled states are generated. In particular, Ng et.al. [35, 36] studied the properties of entanglement with the same model (2). Their studies reveal that the generation of entanglement can occur under the condition either (i) the condensates are symmetric with $4\kappa \gg N\Omega$ [35] or (ii) the condensates are not symmetric with $\Omega \gg \kappa > \kappa_a(\kappa_b)$ [36]. While with these conditions two species of particles are entangled, what characterizes the correlations is not clear. On the other hand, their studies restrict to either strong interaction regime (i) or weak interaction regime (ii) with a large number of particles. Studying the system within an expanding parameters range will help us understand the correlation and entanglement of this system deeply.

A. Von Neumann Entropy

At first we introduce Von Neumann entropy [48] to characterize the degree of entanglement between these two kinds of particles. By obtaining the eigenstates and eigenvalues of Hamiltonian (2), we can calculate the density matrix of the system at any time t

$$\rho_{AB}(t) = |\Phi(t)\rangle\langle\Phi(t)| \quad (14)$$

Then Von Neumann entropy is defined as ($N_a = N_b = N$)

$$S(t) = -\text{tr}[\rho_A(t)\ln\rho_A(t)] = \text{tr}[\rho_B(t)\ln\rho_B(t)] \quad (15)$$

Here $\rho_A(t)$ and $\rho_B(t)$ are reduced density matrices of the respective subsystems

$$\rho_A(t) = \text{tr}_B[\rho_{AB}(t)], \rho_B(t) = \text{tr}_A[\rho_{AB}(t)] \quad (16)$$

Von Neumann entropy describes how much the species are entangled with time. As a result, we can measure the entanglement of these states at given parameters and estimate the maximal value of entanglement of the system. The dimension of the reduced density matrices ρ_A (or ρ_B) is $N_A + 1$ (or $N_B + 1$). When the states of the subsystem have equal probability to be occupied, Von Neumann entropy reaches its maximal value $\ln(N_A + 1)$ or $\ln(N_B + 1)$. In order to condense information about the system's entanglement with various parameters, we characterize Von Neumann entropy by its time average

$$S_{ave} = \frac{1}{\Delta t} \int_0^{\Delta t} dt S(t) \quad (17)$$

employing the averaging interval $\Delta t = 30\Omega t$, which ensures the entropy reaches its saturating values. We start with a Fock state $|j, 0\rangle \equiv |j_a, j_a\rangle_A |j_b, -j_b\rangle_B$, which denotes component A and component B are prepared in right well and left well correspondingly. FIG. (4) depicts results of such calculations. The averaged entropy continuously increase with u until to a maximal value. Then the value of the entropy will not increase but descend slowly. Note in the parameter range we considered here the entropy never reaches to $\ln(N_a + 1)$. It is interesting there is a *jut* in the descending region. An approximated calculation [35] indicates that states of the form $|n, N_a - n\rangle_A |m, N_b - m\rangle_B$ dominates the dynamics due to entanglement as $4\kappa \gg N\Omega$. However, data in FIG. (4) seem to imply particles of two species are entangled adequately even when $4\kappa \ll N\Omega$. Since one prefers to paired tunneling as entanglement, we carefully check the states involved in the dynamics. When $4\kappa \gg N\Omega$, the system is likely to stay the states similar to $|n, N_a - n\rangle_A |m, N_b - m\rangle_B$ while much more other states are excited into the dynamics when $4\kappa \ll N\Omega$. We also study the situation that $\kappa_a = \kappa_b \neq \kappa$ while keep the system in the strong interaction regime. The results indicate

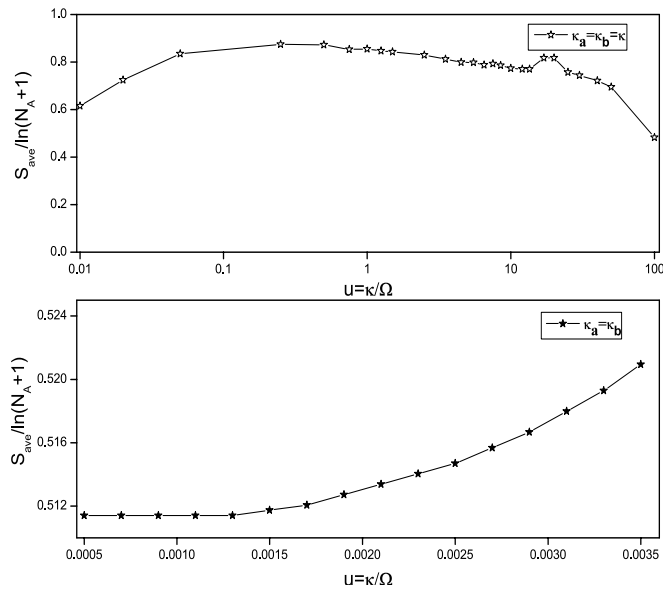


FIG. 4: Normalized entropy for different $u = \Omega/\kappa$ with $N_a = N_b = 20, \Omega_a = \Omega_b = \Omega = 1$. Here we plot normalized entropy $S_{ave}/\ln(N_a + 1)$ of component A. We set $\kappa_a = \kappa_b = \kappa$ (top) and $\kappa_a = \kappa_b = 0.01$ (bottom) accordingly .

that slight difference between $\kappa_a (= \kappa_b)$ and κ will destroy the entanglement of two species. The system collapses to almost a single basis state and consequently Von Neumann entropy oscillates within a small amplitude.

In the so called weak interaction regime [36], we find in a small range Von Neumann entropy, whether $\kappa > \kappa_a = \kappa_b$ or $\kappa < \kappa_a = \kappa_b$, is larger than the case $\kappa = \kappa_a = \kappa_b$. However, the numerical study demonstrates paired tunneling is the major form of the dynamics only when $\kappa > \kappa_a = \kappa_b$ within a small range. Exceeding this range, Von Neumann entropy comes down. See FIG. 4(bottom).

B. Quantum Correlation

Although Von Neumann entropy can be used to quantify the degree of entanglement of two species, it is not sufficient to estimate how the system is entangled. We have shown paired tunneling entanglement and chaotic superposition of states can both contribute to Von Neumann entropy (FIG. 4). But what can be used to distinguish entanglement and chaotic superposition of states has not been addressed.

Here we calculate the second-order correlation function [49] and demonstrate the onset of paired entanglement accompanied by the violation of Cauchy-Schwarz inequality. The single-time two-mode second-order cross-correlation function is bound by the upper bound

$$G_{i,j}^{(2)}(t) \leq \left(G_i^{(2)}(t) G_j^{(2)}(t) \right)^{\frac{1}{2}} \quad (18)$$

We have introduced the single-time two-mode second-order correlation functions

$$G_{i,j}^{(2)}(t) \equiv \langle \Phi(t) | \hat{a}_i^\dagger \hat{a}_i \hat{a}_j^\dagger \hat{a}_j | \Phi(t) \rangle \quad (19)$$

and the single-time, single-mode, second-order correlation functions

$$G_j^{(2)}(t) \equiv \langle \Phi(t) | \hat{a}_j^\dagger \hat{a}_j^\dagger \hat{a}_j \hat{a}_j | \Phi(t) \rangle \quad (20)$$

To examine the correlation, we calculate time dependence of the second-order cross-correlation function between two species in different wells

$$R_{a_L, b_R}^{(2)} \equiv \frac{G_{a_L, b_R}^{(2)}(t)}{\sqrt{G_{a_L}^{(2)}(t) G_{b_R}^{(2)}(t)}} \quad (21)$$

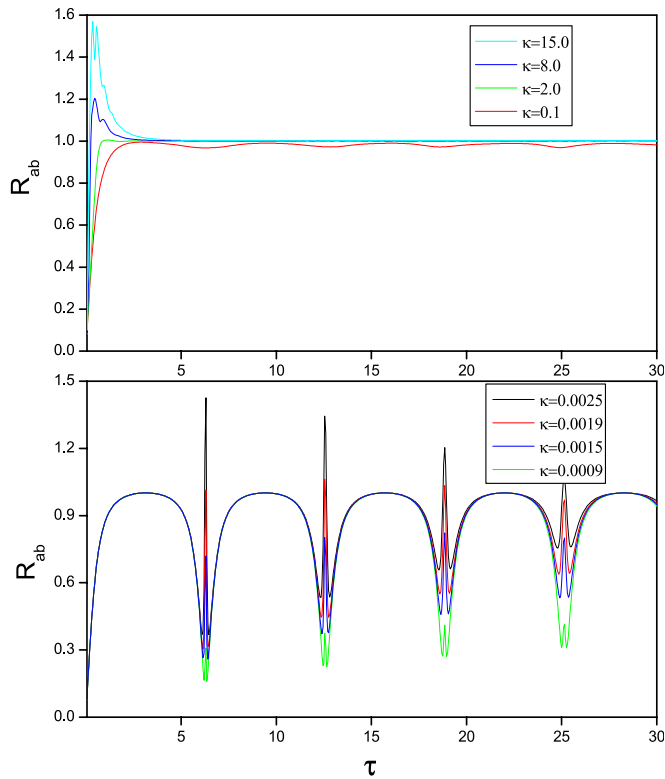


FIG. 5: Normalized second-order cross-correlation function of two species in different wells. The parameter setting is same as FIG. (4).

The results are depicted in FIG. (5). These results illustrate how the correlations between mode a_L and b_R do violate the classical Cauchy-Schwartz inequality when paired tunnelling entanglement is prominent. The violation of second-order two-mode correlation can be well understood by looking at the Von Neumann entropy. Von Neumann entropy can quantify the degree of entanglement of two species, but it can not be used to justify the onset of entanglement. The entanglement of two species can only be triggered when the correlation function is violated. Otherwise the entropy comes from the superposition of all basis states. With the help of second-order cross correlation function, one thus can distinguish whether the system is entangled as well as measure the degree of entanglement by Von Neumann entropy.

V. DISCUSSION AND CONCLUSION

Our systematic approach has shown, for the first time, the onset of avoid level-crossing of two-component BECs system in a double well. Different from the erratic level crossings of a single component system [42], we find the avoided level-crossing always exists even for a intermediate system. As the number of particles of each components increases, the avoided level-crossing happens during a narrower range of $u = \kappa/\Omega$. What interesting is it shares the similar character of the level repulsion of an interacting boson model [43], where the system undergoes a transition from SU(5) to SU(3). Other similar examples include the Floquet spectra of one-dimensional driven systems [50], in which the level-crossings are induced by chaos. Note here our result is exact the energy spectra. Mahmud et.al. [47] have studied the double-well system using phase-space dynamics. Their results reveal even for a very small system (only 4-8 particles per well) the classical chaos is manifest for a driven double-well BECs. However, their Hamiltonian is slightly different from ours and their calculation only demonstrates the merging of energy levels. The system considered in this paper is much more complicated than the one containing single component BECs [47]. Although in the highly degenerated region there are apparent signatures of the onset of entanglement [35, 36], in the avoided level-crossing region the dynamics has not been addressed clearly. It is not sure such crossing may relate to chaotic dynamics.

One may prefer Von Neumann entropy to quantify the entanglement [35, 36, 38]. Our results imply entropy is not sufficient to quantify whether the entanglement is triggered. However by calculating the second-order crossing corre-

lation function, the dynamics can be obviously classified. In particular, the second-order crossing correlation function will violate Cauchy-Schwarz inequality when the system is entangled. Thus this system is one of the candidates of many-particle entanglement of BECs [30, 35, 36, 38, 46]. On the other hand, in the strong interaction [35] of the system (2), a slightly difference between $\kappa_a = \kappa_b$ and κ will destroy the entanglement of two species. Thus it is hard to implement in a real experiment.

In conclusion, we have studied the quantum dynamics of two-component BECs in double-well thoroughly using the two-mode approximation model [9, 10, 11]. After performing a systemical approach [20, 39, 41] to obtain the eigenvalues of the Hamiltonian (2), we find the energies become to degenerate in the weak and strong interaction regime while undergo avoided level-crossings, which may indicate some other dynamics. The quantum dynamics studies demonstrate the self-trapping effect and oscillation of the system. We show self-trapping of both the whole system and individual component can happen with appropriate conditions. We also study the quantum entanglement and correlation in two extreme situations, i.e. weak interaction regime and strong interaction regime. Our numerical experiments reveal that the onset of entanglement of two species can be signed by the violation of Cauchy-Schwarz inequality of second-order cross correlation function. And the degree of entanglement is thus measured by Von Neumann entropy.

Further perspectives of system (2) include what relates avoided level-crossings and whether it can cause certain kind of chaos [42]. The quantum phase-space method [46, 47] may be a feasible candidate for the study of these problems. And in a real system contains two-component BECs [21, 22, 23], $\kappa_a, \kappa_b, \kappa$ and Ω_a, Ω_b are actually different. What this influences level, dynamics and entanglement may serve an interesting topic.

Acknowledgments

The work is supported in part by the NSF of China (Grant Nos. 60478029, 10125419, 10575040 and 90503010) and by the National Fundamental Research Program of China, Grant No.2005CB724508.

-
- [1] I. Bloch, Nature Physics **1**(2005) 23.
 - [2] M. Greiner, O. Mandel, T. Esslinger, T. W. Häsch, and I. Bloch, Nature **415**(2002) 39.
 - [3] C. Orzel, A. K. Tuchman, M. L. Fensclau, M. Yasuda, and M. A. Kasevich, Science **291**(2001) 2386 .
 - [4] M. Jäskeläinen and P. Meystre, Phys. Rev. A, **71**(2005) 043603
 - [5] D. Jaksch et al., Phys. Rev. Lett. **82**(1999) 1975 .
 - [6] I. Bloch, Phys. World **17**(2004) 25.
 - [7] M. P. A. Fisher, P. B. Weichman, G. Grinstein, and D. S. Fisher, Phys. Rev. B **40**(1989) 546 .
 - [8] D. Jaksch, C. Bruder, J. I. Cirac, C. W. Gardiner, and P. Zoller, Phys. Rev. Lett. **81**(1998) 3108.
 - [9] G. J. Milburn, J. Corney, E. M. Wright, and D. F. Walls, Phys. Rev. A **55**(1997) 4318 .
 - [10] M. J. Steel and M. J. Collett, Phys. Rev. A **57**(1998)2920
 - [11] R. W. Spekkens and J. E. Sipe, Phys. Rev. A **59**(1999) 3868 .
 - [12] J. Javanainen and M. Yu. Ivanov, Phys. Rev. A **60**(1999) 2351
 - [13] A. J. Leggett, Rev. Mod. Phys. **73**(2001) 307 .
 - [14] S. Raghavan, A. Smerzi, S. Fantoni, and S. R. Shenoy, Phys. Rev. A **59**(1999) 620 ; A. Smerzi, S. Fantoni, S. Giovanazzi, and S. R. Shenoy, Phys. Rev. Lett. **79**(1997) 4950
 - [15] M. Albiez, R. Gati, J. Fölling, S. Hunsmann, M. Cristiani, and M. K. Oberthaler, Phys. Rev. Lett. **95**(2005) 010402
 - [16] J.E. Williams, Phys. Rev. A **64**(2001) 013610 .
 - [17] R. W. Robinett, Phys. Rep. **392**(2004) 1
 - [18] Julien Vidal, Guillaume Palacios, and Claude Aslangul, Phys. Rev. A **70** (2004) 062304 and references therein.
 - [19] G. Kalosakas and A.R. Bishop, Phys. Rev. A **65**(2002) 043616
 - [20] Y. Wu and X. Yang, Phys. Rev. A **68**(2003) 013608 .
 - [21] D. M. Stamper-Kurn, M. R. Andrews, A. P. Chikkatur, S. Inouye, H.-J. Miesner, J. Stenger and W. Ketterle, Phys. Rev. Lett. **80**(1998) 2027
 - [22] D. S. Hall, M. R. Matthews, J. R. Ensher, C. E. Wieman and E. A. Cornell, Phys. Rev. Lett. **81**(1998) 1539
 - [23] M. Modugno, F. Dalfovo, C. Fort, P. Maddaloni and F. Minardi, Phys. Rev. A **62**(2000) 063607
 - [24] K.V. Krutitsky and R. Graham, Phys. Rev. Lett. **91**(2003) 240406
 - [25] Elena A. Ostrovskaya and Yuri S. Kivshar, Phys. Rev. Lett. **92**(2004) 180405
 - [26] H. T. Ng, C. K. Law and P. T. Leung, Phys. Rev. A **68**(2003) 013604
 - [27] O. Mandel, M. Greiner, A. Widera, T. Rom, T. W. Hänsch, and I. Bloch, Phys. Rev. Lett. **91**(2003) 010407 .
 - [28] G.-H. Chen and Y.-S. Wu, Phys. Rev. A **67**(2003) 013606 .
 - [29] E. Demler and F. Zhou, Phys. Rev. Lett. **88**(2002) 163001 .
 - [30] L. You, Phys. Rev. Lett. **90**(2003) 030402 .

- [31] S. K. Yip, Phys. Rev. Lett. **90**(2003) 250402 .
- [32] B. Damski, L. Santos, E. Tiemann, M. Lewenstein, S. Kotochigova, P. Julienne, and P. Zoller, Phys. Rev. Lett. **90**(2003) 110401 .
- [33] M. G. Moore and H. R. Sadeghpour, Phys. Rev. A **67**(2003) 041603(R) .
- [34] Sahel Ashhab and Carlos Lobo, Phys. Rev. A **66**(2002) 13609 .
- [35] H. T. Ng, C. K. Law and P. T. Leung, Phys. Rev. A **68**(2003) 013604 .
- [36] H. T. Ng and P. T. Leung, Phys. Rev. A **71**(2005) 013601 .
- [37] T. Guhr, A. Müller-Groeling, and H. A. Weidenmüller, Phys. Rep. **299**(1998)189
- [38] J. Chen, Y. Guo, H. Gao and H. Song, arxiv:quant-ph/050719 (2005)
- [39] Y. Wu, X. Yang and Y. Xiao, Phys. Rev. Lett. **86**(2001) 2200
- [40] V. A. Andreev and O. A. Ivanova, J. Phys. A **35**(2002) 8587 .
- [41] Here we list the MATHEMATICA code:
`<<LinearAlgebra`MatrixManipulation`; H = Na; L = Nb; u=Table[Ωa/2((H-i)KroneckerDelta[i, k-1]+i * KroneckerDelta[i, k+1])KroneckerDelta[j, l]+Ωb/2((L-j)KroneckerDelta[j, l-1]+j* KroneckerDelta[j, l+1])KroneckerDelta[i, k]], {k, 0, H}, {i, 0, H}, {l, 0, L}, {j, 0, L}]; v1=BlockMatrix[u]; v2=BlockMatrix[u2]IdentityMatrix[(H+1)(L+1)]; V=v1+v2; e=Eigenvalues[V]; F=Eigenvectors[V];`
- [42] Ying Wu and Xiaoxue Yang, will be published by Optics Letters.
- [43] J.M. Arias, J. Dukelsky, and J. E. García-Ramos, Phys. Rev. Lett. **91**(2003) 162502.
- [44] G. Modugno et al., Phys. Rev. Lett. **89**(2002) 190404 .
- [45] A. Simoni et al., Phys. Rev. Lett. **90**(2003) 163202 .
- [46] A. Micheli, D. Jaksch, J. I. Cirac, and P. Zoller, Phys. Rev. A, **67**(2003) 013607
- [47] K. W. Mahmud, H. Perry, and W. P. Reinhardt, Phys. Rev. A **71**(2005) 023615
- [48] A. Peres, *Quantum Theory: Concepts and Methods* (Kluwer Academic, Dordrecht, 1995).
- [49] D. F. Walls and G. J. Milburn, *Quantum Optics*. Springer Verlag, Berlin, 1994.
- [50] M. Latka, P. Grigolini, and B. J. West, Phys. Rev. A **50**(1994) 1071.